Electronic Supplementary Information for

Intrinsic Auxeticity and Negative Piezoelectricity in Two-dimensional Group-IV dipnictide monolayers with In-plane Anisotropy †

Yue Zhao,[bc] Gaoyang Gou,*[ac] Xiaoli Lu,[bc] and Yue Hao,*[bc]

[a] *Frontier Institute of Science and Technology, and State Key Laboratory for Mechanical Behavior of Materials, Xi'an Jiaotong University, Xi' an 710049, China. E-mail: gougaoyang@mail.xjtu.edu.cn*

[b] *China State Key Discipline Laboratory of Wide Band Gap Semiconductor Technology, Shaanxi Joint Key Laboratory of Graphene, Advanced Interdisciplinary Research Center for Flexible Electronics, School of Microelectronics, Xidian University, Xi'an 710071, China; E-mail:yhao@xidian.edu.cn*

[c] *Collaborative Innovation Center of Quantum Information of Shaanxi Province, Xidian University, Xi'an 710071, China*

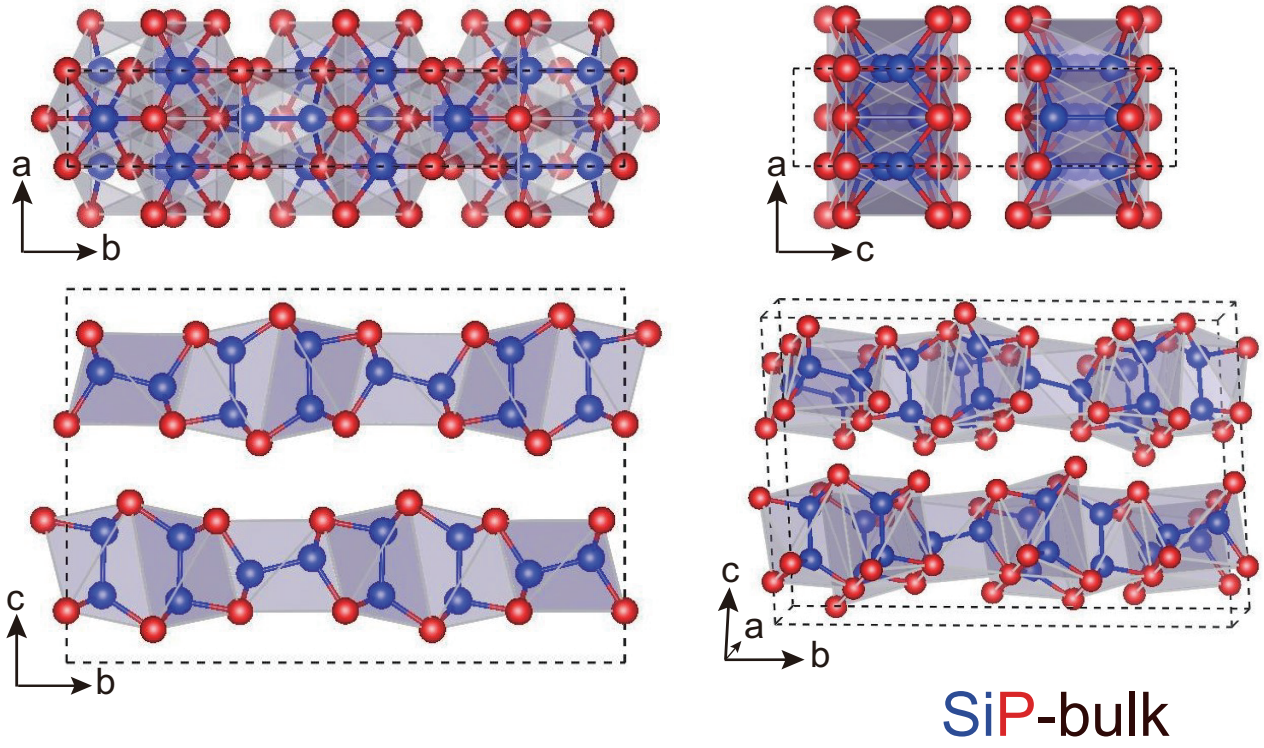

Figure S1: Crystal structure for 3D bulk SiP in orthorhombic $Cmc2_1$ symmetry. Unit cell of bulk SiP is indicated by dashed lines. Si and P atoms are marked in blue and red colors, respectively.

Table S1: Comparison of our calculated (Cal) lattice parameters with experimental (Exp)[1–6] results for all AB and AB_2 (A = Si and Ge, B = P and As) bulk compounds.

		a (Å)	b (Å)	c (Å)	Symmetry	β
GeP	Cal	15.16	3.62	9.15	$C2/m$	101.1°
	Exp	15.44	3.64	9.19	$C2/m$	101.1°
GeAs	Cal	15.53	3.78	9.45	$C2/m$	100.7°
	Exp	15.59	3.79	9.49	$C2/m$	101.3°
SiAs	Cal	16.04	3.66	9.53	$C2/m$	106.1°
	Exp	15.98	3.67	9.53	$C2/m$	106.0°
SiP	Cal	13.69	3.51	20.46	$Cmc2_1$	90°
	Exp	13.96	3.54	20.85	$Cmc2_1$	90°
GeP_2	Cal	14.33	3.49	9.91	$Pbam$	
	Exp	NA	NA	NA		
$GeAs_2$	Cal	14.75	3.72	10.13	$Pbam$	
	Exp	14.76	3.73	10.16	$Pbam$	
SiP_2	Cal	14.38	3.42	9.84	$Pbam$	
	Exp	13.97	3.44	10.08	$Pbam$	
$SiAs_2$	Cal	14.88	3.65	10.07	$Pbam$	
	Exp	14.53	3.64	10.37	$Pbam$	

Table S2: Comparison of our optimized the planar lattice parameters with the results reported by other work for 2D AB and AB_2 monolayers with orthorhombic lattice.

		b (Å)	c (Å)	Symmetry
GeP	Ours	3.59	21.07	C2/m
	Others	3.648[7]	21.393[7]	C2/m
GeAs	Ours	3.73	21.75	C2/m
	Others	3.803,[7] 3.78[8]	22.129,[7] 22.07[8]	C2/m
SiP	Ours	3.50	20.35	C2/m
	Others	3.519,[7] 3.521[9]	20.449,[7] 20.479[9]	C2/m
SiAs	Ours	3.65	21.08	C2/m
	Others	3.682,[7] 3.66[8]	21.246,[7] 21.19[8]	C2/m
GeP_2	Ours	3.48	10.15	$Pmc2_1$
	Others	3.53,[10] 3.522[11]	10.51,[10] 10.205[11]	$Pmc2_1$
$GeAs_2$	Ours	3.69	10.32	$Pmc2_1$
	Others	3.761[11]	10.398[11]	$Pmc2_1$
SiP_2	Ours	3.42	10.04	$Pmc2_1$
	Others	3.442[11]	10.045[11]	$Pmc2_1$
$SiAs_2$	Ours	3.63	10.29	$Pmc2_1$
	Others	3.674[11]	10.300[11]	$Pmc2_1$

Table S3: The summary of the predicted in-plane NPR for single-layer (SL) $PdSe_2$,[12] SL $GaPS_4$,[13] penta-graphene,[14] SL Ag_2S,[15] SL Mo_2C,[16] Be_5C_2,[17] penta-B_4N_2,[18] SL Se_3P_2,[19] 2D VF_4,[20] δ-phosphorene,[21] δ -V^AN (V^A = P, As, Sb, Bi),[22] SL $SiAs_2$, W_2C[23] and $TcTe_2$.[24] Those 2D materials synthesized either in 3D vdW bulk or 2D layered structural forms in experiment are marked by *. $SiAs_2$ monolayer characterizes the in-plane NPR of largest magnitude among all synthetic 2D auxetic materials.

2D materials	In-plane NPR
SL $PdSe_2^*$	-0.022
SL $GaPS_4^*$	-0.033
Penta-graphene	-0.068
SL Ag_2S	-0.12
SL Mo_2C^*	-0.15
Be_5C_2	-0.16
SL Se_3P_2	-0.199
2D $VF_4{}^*$	-0.26
δ-Phosphorene	-0.267
δ-PN	-0.268
δ-AsN	-0.177
δ-SbN	-0.296
δ-BiN	-0.260
SL $SiAs_2^*$	-0.32
$TcTe_2$	-0.37
W_2C	-0.43

Table S4: Comparison of our calculated energy band gaps (E_g in eV) and anisotropic carrier effective masses m_e^*/m_0 and m_h^*/m_0 using HSE06 functional with the results reported by other work for all AB and AB_2 monolayers. The simulated direct and indirect E_g are marked by subscript indices $_D$ and $_I$, respectively.

		m_e^*/m_0		m_h^*/m_0		E_g
		Γ-X	Γ-Y	Γ-X	Γ-Y	
GeP	Ours	0.36	0.72	0.93	0.56	2.48_I
	Others	0.053,[7] 0.40[25]	0.004,[7] 0.72[25]	0.175,[7] 0.98[25]	0.004,[7] 0.57[25]	2.309_I[7]
GeAs	Ours	0.13	0.9	0.78	0.22	2.22_D
	Others	0.118,[7] 0.1328,[8] 0.12[26]	0.004,[7] 0.0178,[8] 0.25[26]	0.152,[7] 0.6221,[8] 0.84[26]	0.002,[7] 0.0068,[8] 0.24[26]	2.077_D,[7] 2.06_I[8]
SiP	Ours	0.14	0.57	1.06	0.73	$2.64_I(2.65_D)$
	Others	0.111,[7] 0.24[9]	0.062,[7] 0.70[9]	0.351,[7] 0.42[9]	0.050,[7] 0.44[9]	2.641_D,[7] 2.59_D[9]
SiAs	Ours	0.11	0.37	0.84	0.22	2.43_D
	Others	0.050,[7] 0.1025,[8] 0.14[26]	0.003,[7] 0.0195,[8] 0.88[26]	0.137,[7] 0.6975,[8] 0.94[26]	0.002,[7] 0.0062,[8] 0.22[26]	2.353_D,[7] 2.50_D[8]
GeP_2	Ours	0.13	1.23	1.39	0.32	$2.08_I(2.10_D)$
	Others	0.14[10]	1.29[10]	1.54[10]	0.38[10]	2.21_I,[10] 1.96_D[11]
$GeAs_2$	Ours	0.13	0.56	0.43	0.63	1.78_I
	Others	NA	NA	NA	NA	1.64_I[11]
SiP_2	Ours	0.12	2.10	3.99	1.12	$2.25_I(2.28_D)$
	Others	NA	NA	NA	NA	2.23_D[11]
$SiAs_2$	Ours	0.13	0.41	0.85	2.20	2.04_I
	Others	NA	NA	NA	NA	1.92_I[11]

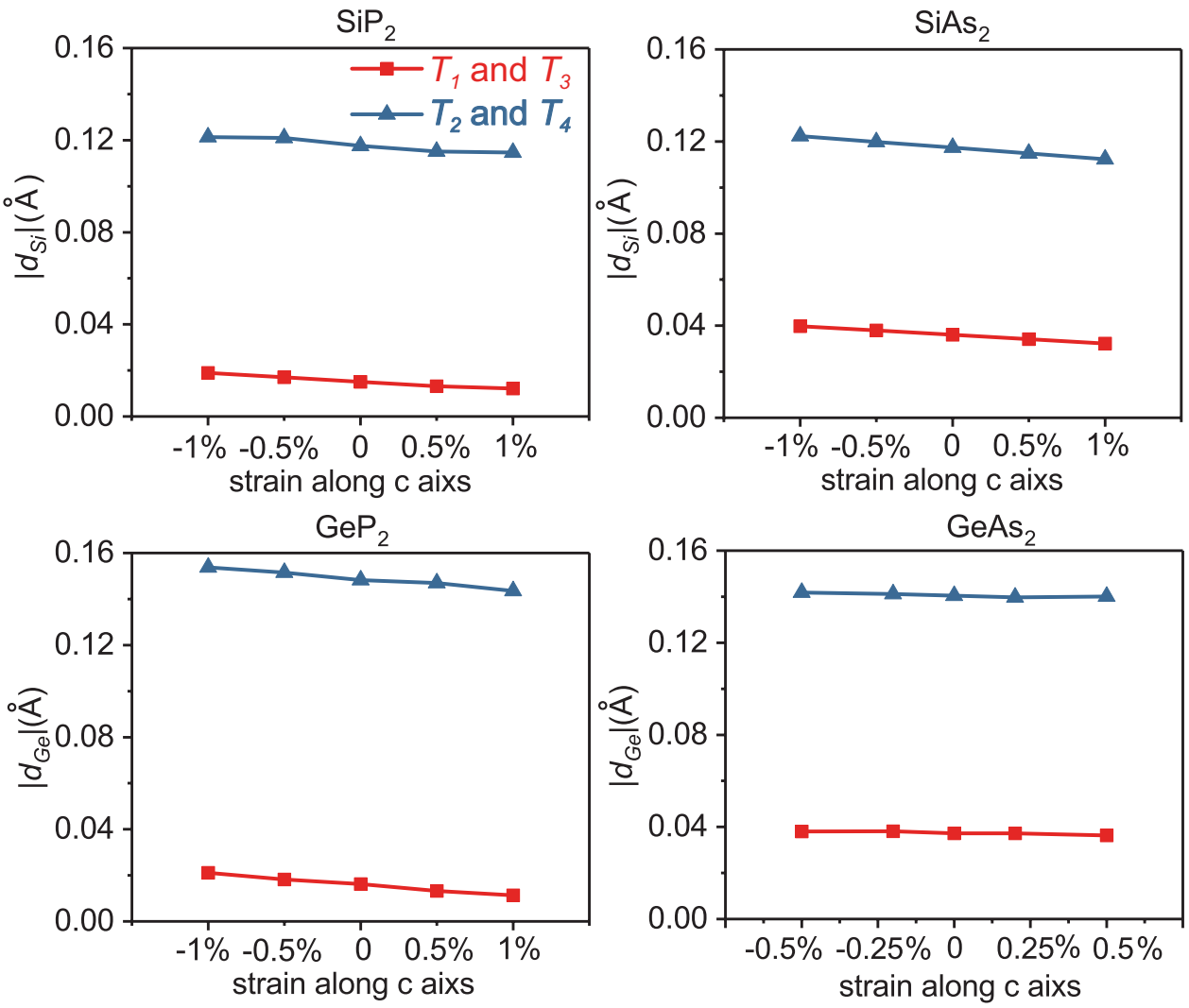

Figure S2: The evolution of cation polar displacement relative to anion tetrahedral center of AB_2 monolayers, as a function of uniaxial strain applied along the polar c axis. Four tetrahedrons (marked as T_1, T_2, T_3, and T_4,) within AB_2 monolayers can yield two distinct polar displacement. Reducing (increasing) the magnitude of polar displacement along the polar c axis by applying tensile (compressive) uniaxial strain will lead to the overall negative piezoelectric coefficients e_{33}^{2D} (d_{33}^{2D}) for AB_2 monolayers.

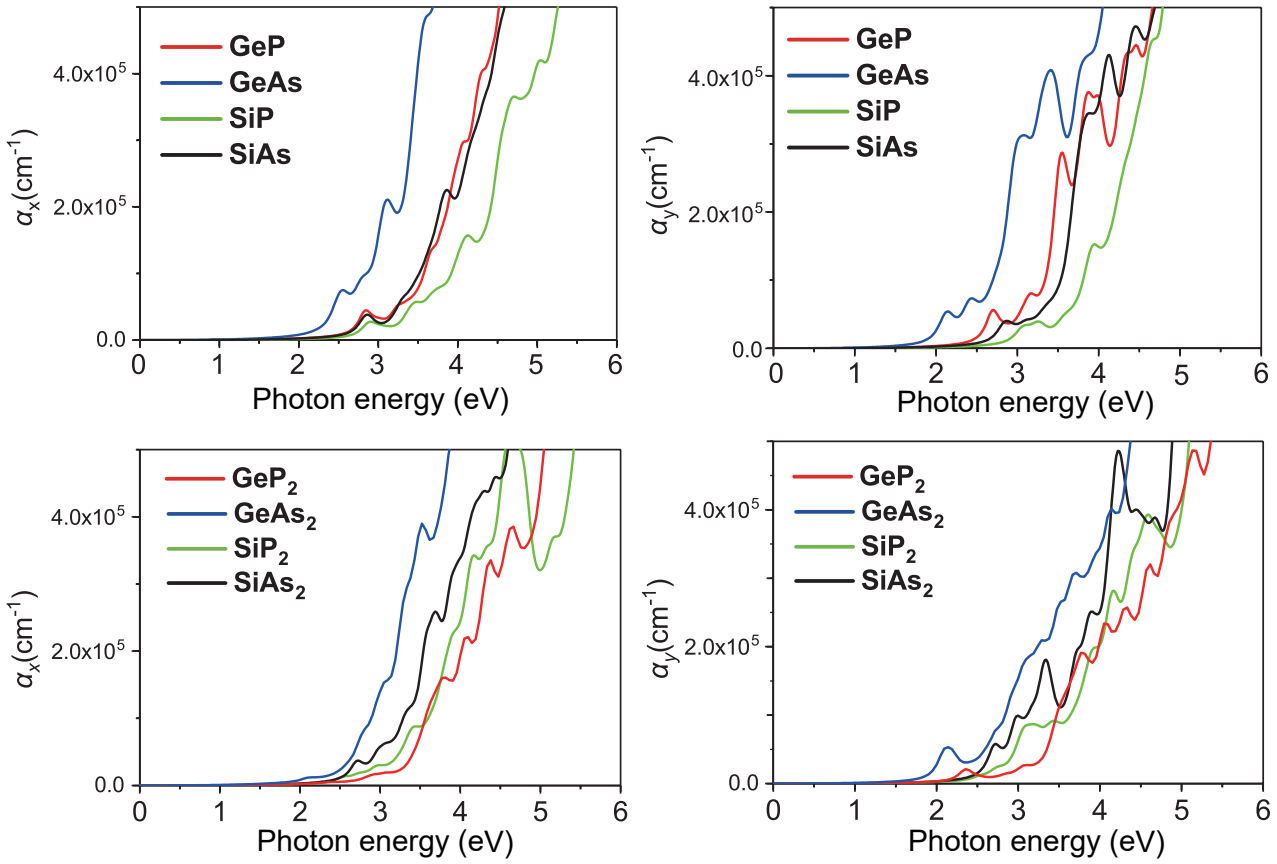

Figure S3: The HSE06 calculations predicted photon energy dependent optical absorption coefficients α_x and α_y for all AB and AB_2 monolayers under incident light polarized along crystallographic b and c axes, respectively.

References

[1] T. Wadsten, *Acta Chem. Scand.*, 1965, **19**, 1232.

[2] T. Wadsten, *Acta Chem. Scand.*, 1967, **21**, 1374.

[3] Y. H. S. Donahue, P. C., *J. Solid State Chem.*, 1970, **1**, 143.

[4] S. H. Bryden, *Acta Crystallogr.*, 1962, **15**, 167.

[5] A. S. Spring-Thorpe, *Mater. Res. Bull.*, 1967, **4**, 125.

[6] S. W. J. G. J. L. Donahue, P. C., *J. Phys. Chem. Solids*, 1968, **29**, 807.

[7] A.-Q. Cheng, Z. He, J. Zhao, H. Zeng and R.-S. Chen, *ACS Appl. Mater. Interfaces*, 2018, **10**, 5133–5139.

[8] L. Zhou, Y. Guo and J. Zhao, *Phys. E*, 2018, **95**, 149–153.

[9] S. Zhang, S. Guo, Y. Huang, Z. Zhu, B. Cai, M. Xie, W. Zhou and H. Zeng, *2D Mater.*, 2017, **4**, 015030.

[10] P. Li, W. Zhang, D. Li, C. Liang and X. C. Zeng, *ACS Appl. Mater. Interfaces*, 2018, **10**, 19897–19905.

[11] Y. Xu, Z. Li, C. He, J. Li, T. Ouyang, C. Zhang, C. Tang and J. Zhong, *Appl. Phys. Lett.*, 2020, **116**, 023103.

[12] G. Liu, Q. Zeng, P. Zhu, R. Quhe and P. Lu, *Comput. Mater. Sci.*, 2019, **160**, 309–314.

[13] J. Yuan, K. Xue, J. Wang and X. Miao, *J. Phys. Chem. Lett.*, 2019, **10**, 4455–4462.

[14] S. Zhang, J. Zhou, Q. Wang, X. Chen, Y. Kawazoe and P. Jena, *Proc. Natl. Acad. Sci.*, 2015, **112**, 2372–2377.

[15] R. Peng, Y. Ma, Z. He, B. Huang, L. Kou and Y. Dai, *Nano Lett.*, 2019, **19**, 1227–1233.

[16] B. Mortazavi, M. Shahrokhi, M. Makaremi and T. Rabczuk, *Nanotechnol.*, 2017, **28**, 115705.

[17] Y. Wang, F. Li, Y. Li and Z. Chen, *Nat. Commun.*, 2016, **7**, 11488.

[18] M. Yagmurcukardes, H. Sahin, J. Kang, E. Torun, F. M. Peeters and R. T. Senger, *J. Appl. Phys.*, 2015, **118**, 104303.

[19] Y. Chen, X. Liao, X. Shi, H. Xiao, Y. Liu and X. Chen, *Phys. Chem. Chem. Phys.*, 2019, **21**, 5916–5924.

[20] L. Zhang, C. Tang and A. Du, *J. Mater. Chem. C*, 2021, **9**, 95–100.

[21] H. Wang, X. Li, P. Li and J. Yang, *Nanoscale*, 2017, **9**, 850–855.

[22] W. Xiao, G. Xiao, Q. Rong and L. Wang, *Phys. Chem. Chem. Phys.*, 2018, **20**, 22027–22037.

[23] D. Wu, S. Wang, S. Zhang, J. Yuan, B. Yang and H. Chen, *Phys. Chem. Chem. Phys.*, 2018, **20**, 18924–18930.

[24] L. Yu, Q. Yan and A. Ruzsinszky, *Nat. Commun.*, 2017, **8**, 15224.

[25] L. Li, W. Wang, P. Gong, X. Zhu, B. Deng, X. Shi, G. Gao, H. Li and T. Zhai, *Adv. Mater.*, 2018, **30**, 1706771.

[26] P. Li, W. Wu, Y. Xu, J. Liu, S. Wu, Y. Ye, C. Liang and X. C. Zeng, *J. Phys. Chem. Lett.*, 2021, **12**, 1058–1065.